Egyptian Sugar Journal(2024), 22: 69 - 79
https://doi.org/10.21608/esugj.2024.309772.1068

RESEARCH ARTICLE

Synthesis of Fe_3O_4@BAMTM for removing inorganic and organic contaminants from an aqueous solution: Screening and optimization

Ahmad Abo Markeb,[1*] Abdelreheem Abdelfatah Saddik,[2*] Ahmed Abdelrahim M.Elgaffary, [3*] Adel M Kamal El-Dean[1] Abdel-Aal M. Gaber[1]

Received: 4 August 2024\ Revised: 12 August 2024\ Accepted: 18 August 2024\ Published online: 22 August 2024

Abstract

Nowadays, one of the most intriguing challenges in water remediation is the elimination of heavy metals from industrial wastewater using materials that function as adsorbents. This study introduces a new nanocomposite called Fe_3O_4@BAMTM, which serves as an adsorbent and evaluates its effectiveness in removing heavy metals and Coomassie Brilliant Blue (CBB) from wastewater.

The optimization of the adsorption process was carried out using the Box-Behnken Design (BBD) model in conjunction with the Response Surface Methodology (RSM).

The optimal conditions for Coomassie Brilliant Blue (CBB) removal were determined to be a pH 2, a dosage 0.10 g/L, and a temperature 35℃, utilizing the Fe_3O_4@BAMTM NC, which exhibited superior adsorption capabilities, with an adsorption capacity of 555.56 mgCBB/gNC and rapid attainment of adsorption equilibrium (30 minutes). Furthermore, the Fe_3O_4@BAMTM demonstrated 67% and 65% removal of iron (III) and nitrate ions, respectively, from the wastewater.

Keywords: Synthesis; Fe_3O_4@BAMTM Nanocomposite; Adsorption; Wastewater

[1] Chemistry Department, Faculty of Science, Assiut University, 71516-Assiut, Egypt
[2] Materials Science and Engineering Lab., Department of Chemistry, Faculty of Science, Assiut University, 71516-Assiut, Egypt
[3] Department of Environmental Science and Pollution Treatment, Faculty of Sugar and Integrated Industries Technology, Assiut University, Assiut, Egypt
* Ahmad Abo Markeb and Abdelreheem Abdelfatah Saddik equally contributed to this work.
*corresponding author; mido5lord@gmail.com.

Introduction

Water is crucial for sustaining life, playing a vital role in public health and community well-being. Accessibility to clean and safe water is a fundamental aspect of maintaining a healthy society (Kılıç 2020).

Throughout history, impurities in water have frequently resulted in outbreaks of waterborne diseases, causing immediate and long-lasting health issues ranging from diarrhea to loss of life (Shayo et al. 2023).

Contaminated water is often the primary pathway through which humans are exposed to infectious pathogens and harmful organic and inorganic substances that can cause cancer.

In recent decades, the growth of the global population and the effects of globalization have contributed to an increase in waste production and the emergence of various pollutants in water, including pharmaceuticals, hormones, chemicals, viruses, and toxins (Programme United Nations Environment (2016).

Various pollutants exhibit different characteristics and properties. Stock pollutants, including non-biodegradable plastics (Rahman et al. 2021), synthetic chemicals, pesticides, and heavy metals, possess minimal or negligible absorptive capacity.

Consequently, these pollutants accumulate in the environment over time. The detrimental impact of anion toxicity on the environment and human health has gained widespread recognition (Shayo et al. 2023).

Effective management and removal of anions from water bodies have become a central concern across many regions globally.

While a diverse and heterogeneous group of anions, including (NO^{3-}, $SO^{4-}2$, $PO4^{-3}$, etc.), contributes to these issues, certain anionic species are particularly significant due to their associated health risks. Consequently, considerable efforts have been dedicated to eliminating these anions from water sources such as rivers, lakes, and groundwater.

On the other hand, heavy metal pollutants encompass metallic and metalloid elements with high density (ranging from 3.5 to 7 g/cm3), which are toxic or harmful even at low concentrations.

These elements include mercury (Hg), cadmium (Cd), arsenic (As), chromium (Cr), thallium (Tl), zinc (Zn), nickel (Ni), copper (Cu), and lead (Pb). They are widely distributed in the Earth's crust and are non-biodegradable.

They enter the human body through air, water, and food. While a few of these metals play a crucial role in human and animal metabolism in trace amounts, higher concentrations can lead to toxicity and health risks. Additionally, nanotechnology presents new possibilities for water purification, with examples such as nanoparticles (NPs), nanomembranes, carbon nanotubes (CNTs), and nanofibers. Consequently, adsorbent nanomaterials have emerged as an intriguing method for removing various contaminants from drinking water, including heavy metals and, to a lesser extent, nutrients (Mahmood et al. 2015).

Over the past decade, numerous applications involving nitrogen-containing heterocyclic compounds have been reported. These compounds, particularly s-triazoles connected to heterocyclic rings, have shown diverse biological activities, biomedical uses, and commercial applications like dyes, insecticides, and herbicides. Recently, there has been significant interest in s-triazoles and their fused heterocyclic derivatives due to their notable medicinal significance (Dad et al. 2022).

Many well-known drugs, such as triazolam, alprazolam, and etizolam, incorporate the s-triazole group. Additionally, the triazole moiety exhibits potential in various therapeutic activities, including antiviral, anthelmintic, antitumor, anti-inflammatory, antitubercular, and analgesic effects (Kerru et al. 2020).

Hence, adsorption technology has gained extensive use in removing heavy metals and other contaminants from water due to its cost-effectiveness, ease of operation, and environmental friendliness.

Using adsorbent nanomaterials for heavy metal removal is highly advantageous because of increased active sites and a larger specific surface area for contaminant adsorption (Njum 2017). Various adsorbent materials, including resins, activated carbon, biomaterials, and agricultural byproducts, have been employed to eliminate pollutants from water. However, these materials have drawbacks such as low adsorption capacity, selectivity, separation difficulties, reusability, and stability when used for Iron (III) removal. Consequently, this study aims to synthesize newnanocomposites (NCs), specifically Fe_3O_4@BAMTM, using bis (4-amino-5-mercapto-1,2,4-triazol-3-yl) methane (BAMTM) with strong magnetic properties, characterize the synthesized nanocomposites through various techniques to determine their efficiency for iron(III) ion removal, including morphology, size, stability, and crystallinity, and optimize the removal and adsorption capacity of iron (III) ions on Fe_3O_4@BAMTM NCs using the Response Surface Methodology (RSM) with a Box-Behnken Design (BBD) (Ciğeroğlu et al. 2024).

Experimental

Materials

Potassium hydroxide (KOH), absolute ethanol, hydrazide hydrate (80%), carbon disulfide (CS_2), dry diethylether, dimethylformamide (DMF), diethyl malonate, sodium phosphate, sodium sulfate, sodium nitrate, ammonia, manganese nitrate, zinc nitrate, copper nitrate,sodium hydroxide (NaOH),Iron (II) chloride ($FeCl_2$), iron(III) chloride hexahydrate ($FeCl_3.6H_2O$),lead nitrate ($PbCl_2$), and cadmium nitrate ($CdCl_2$), were purchased from SigmaAldrich, Germany. All solutions were prepared with Milli-Q water and filtered using a 0.45 µm Nylon membrane filter.

Synthesis of bis (4-amino-5-mercapto-1,2,4-triazol-3-yl) methane(BAMTM)

Bis (4-amino-5-mercapto-1,2,4-triazol-3-yl) methane was prepared according to the literature.(2) and (3). Asuspension of bis-potassium dithiocarbazinate (1 mmol,0.3g) in water (5 mL) and hydrazine hydrate (80%, 3 mmol) was heated for 18– 20 h at 100°C with occasional shaking. The color of the reaction mixture changed to green with the evolution of hydrogen sulfide gas. After that, the reaction mixture was cooled to room temperature, diluted with cold water (20 mL), and acidified with dil. HCl. The required triazole was precipitated and recrystallized with a DMF water mixture (Mustafa et al. 2012).

Synthesis of Fe_3O_4@BAMTM nancomposites

First, $FeCl_2$ and $FeCl_3 \cdot 6H_2O$, with a Fe^{2+}/Fe^{3+} molar ratio of 1:2, were dissolved in 100 mL of deoxygenated ultrapure water (Milli-Q) containing 0.1% of acetyl trimethyl ammonium bromide. Then, the suspension was incubated for 1 hr. at 40 °C and under an Argon atmosphere. Secondly, 0.6 M NaOH solution was titrated into the iron salt solution under agitation until pH 9.0 was achieved. During titration, the mixture's color turned from light yellow to red-brown and eventually black, confirming the formation of Fe_3O_4-NPs. Then, the suspension containing Fe_3O_4-NPs was incubated for 1 hr. under Argon at 40 °C. Afterward, the NPs were washed three times using ultrapure water and magnetic decantation.

Characterization of Fe_3O_4@BAMTM NCs

High-Resolution Transmission Electron Microscopy.

The nanocomposite characterizations: the morphology and size of the NPs were characterized using a JEM-2011/JEOL, High-Resolution Transmission Electron Microscopy (HR-TEM) equipped. Measurements were acquired with an Oxford INCA X-MAX detector. Different TEM images were studied with Image software to evaluate the NPs average sizes (11) and (12).

Fourier Transform Infrared spectra (FT-IR)

Fourier Transform Infrared spectra (FT-IR) were measured using Shimadzu- 470, in the wavenumber range of 400 – 4000 cm^{-1} with accuracy ± 0.01 cm^{-1} using the KBr disc technique, to determine different functional groups contained in the synthesized sample.

X-Ray diffraction analysis (XRD)

XRD technique was used to obtain the crystalline structure of the Fe_3O_4@BAMTM. Diffraction patterns were collected on PanalyticalX´Pert PRO MPD (Multipurpose Diffractometer).

Zeta potential measurements

The zeta potential of the synthesized nanocomposite (1.0 g/L) was measured using the Zetasizer (Malvern UK).

Adsorption studies

The synthesized composites were used in a batch operation mode to remove dyes, anions, and cations from aqueous solutions and determine the optimal conditions for maximum removal efficiency and adsorption capacity (Liu et al. 2010). A specific amount of the adsorbent (in milligrams) was mixed with a known volume (VL) and concentration (in mg/L) of metal solutions at a defined pH, using an incubating shaker (JSR, Korea) at 180 revolutions per minute for a specified duration (in minutes) (Gulyás et al. 2023).

Subsequently, the remaining concentration of metal solutions (C_e) was measured using Atomic Absorption Spectroscopy (AAS) (Contra AA 700, Germany) after digesting the sample in a 5% HNO_3 solution for 24 hr. or using a UV/VIS spectrophotometer (PG990 Instruments, UK) after separating the adsorbent through magnetic separation with a neodymium magnet. Cations were analyzed using Inductive Coupled Plasma coupled to Optical Emission Spectroscopy (ICP-OES) and Atomic Absorption Spectroscopy coupled to Thermal Decomposition (Khuri et al. 2010). Dyes and anions were determined by spectrophotometry using a Cary 60 UV-VIS spectrophotometer, Agilent, Germany. The removal efficiency (R, %) and the adsorption capacity (Q, mg/g) were calculated using the following equations (Equations 1 and 2):

$$R\ (\%) = \frac{(C_o - C_e)x\ 100}{C_o}$$

$$Q\ (mg/g) = \frac{(C_o - C_e)x\ V_L}{m_g}$$

Where $C_o$and C_e are the concentration of metal ions before and after adsorption, respectively.V_L, and mg are the volume of solution containing adsorbate in liters and the weight of the adsorbent in grams (Ostertagova et al. (2012).

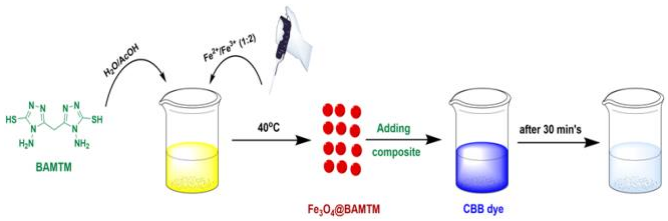

Figure 1. Graphical representation for our study.

Optimization parameters of dye removal

Response Surface Methodology (RSM)

The response surface methodology (RSM) was used to determine the relationship between groups of test factors to determine the optimum conditions. So, the experimental data obtained from CCD were analyzed by RSM and then the mathematical model (Sawyer et al. 2009).

Significant factors were determined using an experiment design to invest time and cost.

A response surface methodology (RSM) model was employed to optimize the removal of dyes. Three independent variables were investigated: pH, amount of Fe_3O_4@BAMTM and temperature (Zhang et al. (2016).

The design consists of three levels (low, medium, and high), coded as (-1,0,+1), and with a total of 17 runs, as shown in Table 1. The experimental data were analyzed using Design Expert software (version 6.0.6, STATEASE Inc., USA).

Factors	Low level (-1)	Medium level (0)	Highest level (+1)
pH	2	6	10
Dose, g/L	0.1	0.8	1.5
Temperature, ℃	20	35	50

Table 1. Independent variables and levels used in CCD

Statistical analysis

The most common model used is quadratic, representing a second-order polynomial equation to fit the experimental data, as shown in Equation 3.

$$Y = \beta_0 + \sum_{i=1}^{k} \beta_i X_i + \sum_{i=1}^{k} \beta_{ii} X_i^2 + \sum_{i=1}^{k-1} \sum_{j=2}^{k} \beta_{ij} X_i X_j$$

(Equation 3)

Where Y is the response, xi, xj, …., xk are the input variables, β0 is the intercept term, βi(i=1, 2, …, k) is the linear effect, βii (i=1, 2, …, k) is the squared effect, and βij(i=1, 2, …, k, j= 1, 2, …, k) is the interaction effect (Sawyer et al. 2009).

The analysis of variance (ANOVA) was employed to justify the significance and competence of the developed regression model. The competence of the RSM model was validated by calculating the correlation coefficients (R_2), adequate precision, and lack of fit (Mahmoud et al. 2011).

Results and Discussion

Morphologicaland structural characterization of the synthesized nanocomposite of the magnetic nanocomposite

High-Resolution Transmission Electron Microscopy analysis

The morphology of the Fe_3O_4@BAMTM NC was determined using High-Resolution Transmission Electron Microscopy and is shown in Figure 2. The nanocomposite was observed to have two shapes, cubic and rods, as shown in Figure 2a. The cubic shape could be attributed to the magnetite nanoparticles (NPs) (Mahmoud et al. 2011) and the rod shape could be attributed to the organic moiety.

The size of the cubic NPs was found to be in the range of 8.26 nm to 12.10 nm, and the length of the rods ranged from 84.84 nm to 211.22 nm with a width of 9.17 nm to 17.11 nm. Moreover, the selected area diffraction pattern of the synthesized nanocomposite is shown in Figure 2b. It can be observed that a crystalline nanomaterial was obtained due to the presence of the white ring.

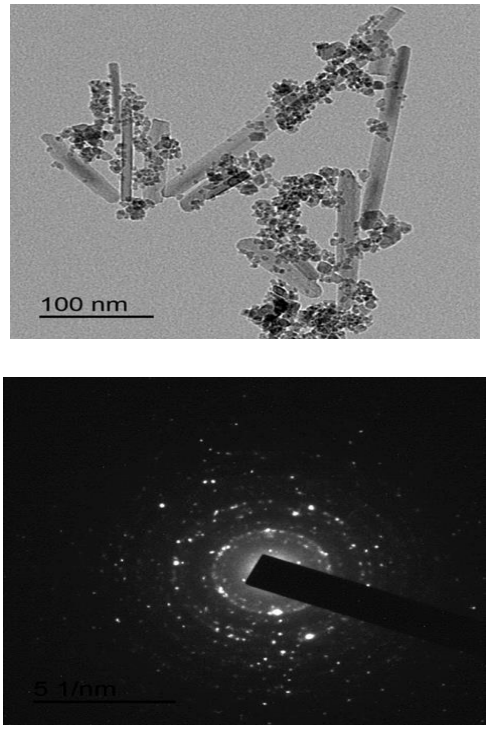

Figure 2. HR-TEM and SAED images of the Fe_3O_4@BAMTM.

XRD analysis

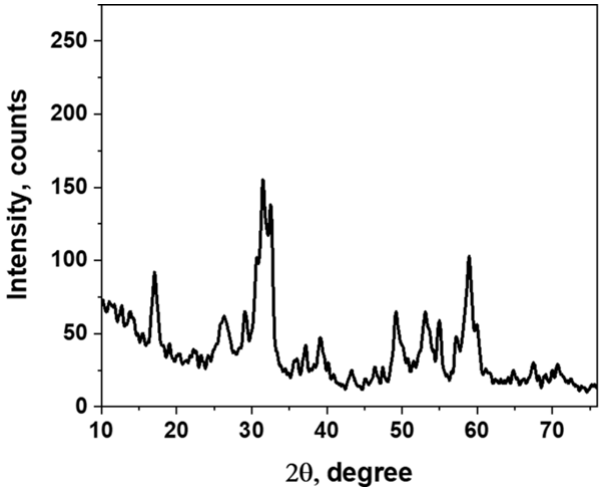

Figure 3.XRD patternof the synthesized nanocomposites.

In order to perform an X-ray powder diffraction experiment, the sample has to be brought to the powder phase. This was accomplished by maintaining 0.5 ml of the liquid sample, as described in the previous section at 85oC for 2 hr. till it became a black solid sample. It was removed from the bottom of the Petri dish with a cutter blade and deposited in the sample holder of the X-ray diffractometer. The measurement was performed in the range angle 2θ=10-750 and in a step-scanning mode of 0.02. A pure corundum powder standard sample was used to correct the data for instrumental broadening. The XRD patterns of the investigated samples were used for crystal phase analysis. Phase analysis was carried out using the unit cell parameters calculated through structure refinement using the Panalytical X'Pert High Score Software (Mohamed et al. 2024).

The microstructural information obtained by single X-ray profile Fourier analysis of the magnetite Fe_3O_4 - cubic crystalline phase were the effective crystallite mean size, Deff (nm) and the root mean square (rms) of the microstrains, 1/2m. The Panalytical X'Pert High Score Software program processed the Warren-Averbach X-ray Fourier analysis peak profiles. The XRD diffraction pattern, presented in Figure 3, illustrates the fact that the sample obtained in our synthesis conditions is the magnetite, Fe_3O_4, witha cubic crystalline structure phase. The Warren-Averbach X-ray Fourier analysis of the (311) and (333) cubic magnetite Fe_3O_4 diffraction profiles was carried out to determine the microstructural parameters of the magnetite Fe_3O_4 - cubic crystalline phase (Sevim et al. (2024).

FT-IR analysis

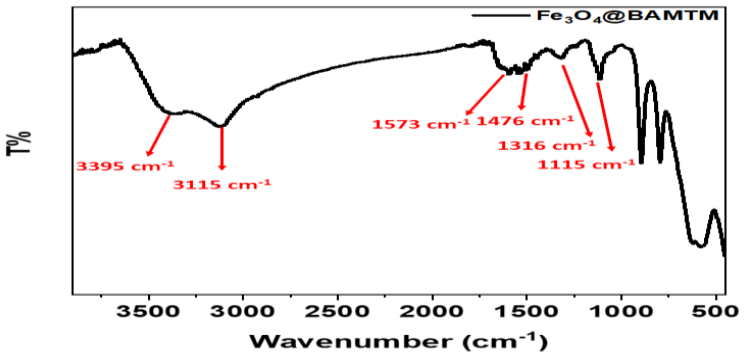

Figure 4.FT-IR analysis of Fe_3O_4@BAMTM nanocomposites

Figure 4 shows the FTIR spectra of Fe_3O_4@BAMTM. The characteristic absorption bands correspond to the synthesized composites' functional groups (26). The strong absorption peaks at 3395 cm-1and 3115 cm^{-1} are attributed to the N-H stretching vibration for NH_2 group. The peaks at 1573 cm^{-1}, 1476 cm^{-1} and 1316 cm-1 correspondto the C=Nstretching vibration. The stretching vibration absorption peak of C=Sappeared at 1115 cm^{-1}(Foo et al.2010).

Zeta potential

Figure 5 presents the net charge of the synthesized nanocomposite by using the zeta potential analysis. It can be shown that the Fe_3O_4@BAMTM NC had a negative charge with a zeta potential of -23.6 mV.

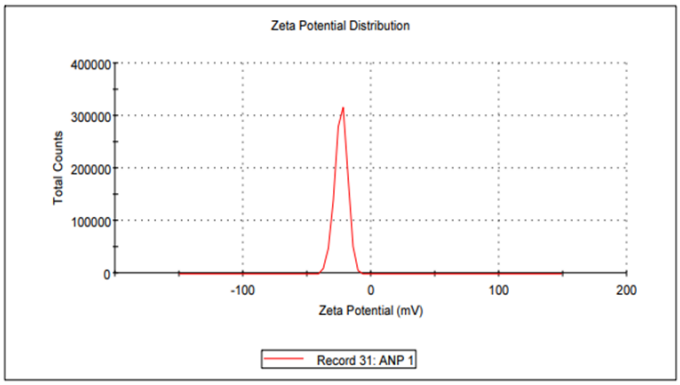

Figure 5. Zeta potentialof Fe_3O_4@BAMTM nanocomposites.

Screening of metal ions, anions, and dyes removal

The efficiency of the synthesized adsorbents toward metals ion removal from solutions of Mg^{2+}, Fe^{3+}, Zn^{2+}, Cu^{2+}, Pd^{2+}, and Cd^{2+} ions by spiking 10.0 mg/Las a concentration which is higher than that it could be found in in the water matrices (Yuan et al. 2019). The results, depicted in Figure 6, exhibit the highest removal efficiency of iron (70%)using Fe_3O_4@BAMTM, followed by copper(II), zinc(II) and lead(II) to 37%, 32 %, and 28 %, respectively. Moreover, lower efficiencies were demonstrated in the case of the manganese (II) (10 %) and cadmium (II) (4 %) ions. Also, the efficacyof the Fe_3O_4@BAMTM was extended to demonstrate the removal of other components from wastewater, suchas nitrate, sulfate, phosphate, and organic dyes, after spiking each contaminant with 100 mg/L, as shown in Figures 7 and 8.

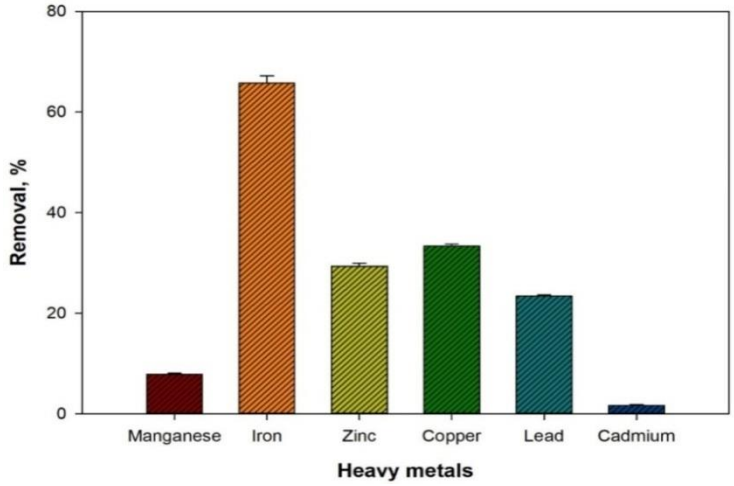

Figure 6. Heavy metal ions removal efficiencies using Fe_3O_4@BAMTM NC.

The maximum removal efficiency was observed in the case of nitrate removal, 70 %. Also, the Fe_3O_4@BAMTM NC shows 52 % and 20 % removal for sulfate and phosphate, respectively. Furthermore, the synthesized adsorbent nanomaterials, Fe_3O_4@BAMTM, showed adsorption of organic dyes from the spiked wastewater. The Fe_3O_4@BAMTM NC showed excellent results towardCoomassie Brilliant Blue (CBB) with removal up to 95% and good result with rosaniline hydrochloride up to 78% removal.

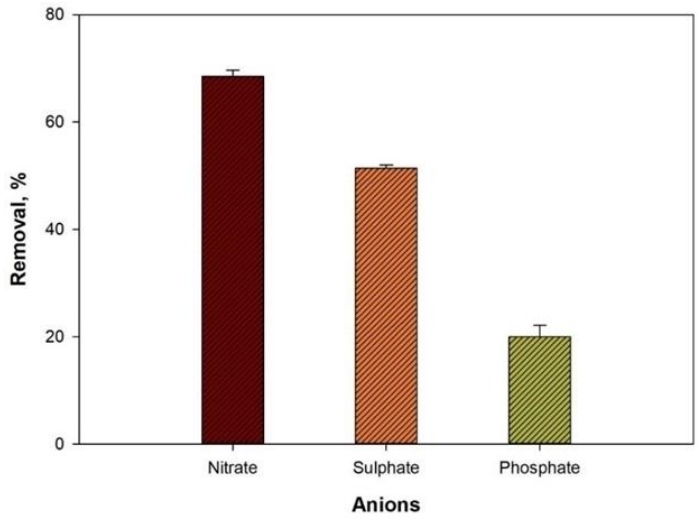

Figure 7. Removal efficiencies of anions (NO_3^-, SO_4^{2-}, andPO_4^{3-}) using Fe_3O_4@BAMTM.

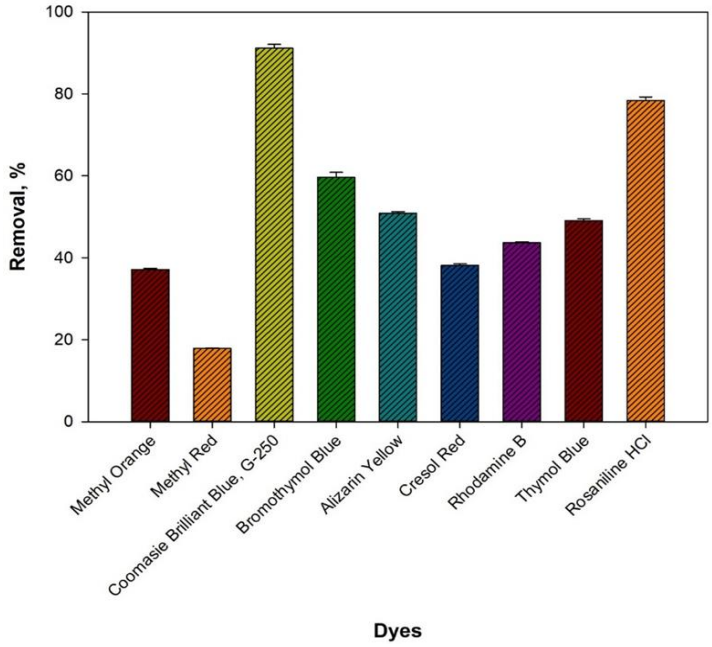

Figure 8. Removal efficiencies of several organic dyes using Fe_3O_4@BAMTM.

Optimization of the Coomassie Brilliant Blue (CBB)removal from aqueous solutions using RSM

The results obtained from the experiment, which utilized the BBD model, can be found in Table 2. The findings indicate that the quadratic model is appropriate for determining the efficiency of Coomassie Brilliant Blue (CBB) dye removal and the adsorption capacity using Fe_3O_4@BAMTM, as shownin the BBD results (Ajala et al. 2019). Table 3 further demonstrates that the quadratic model adequately represents the adsorption capacity and removal efficiency of CBB using Fe_3O_4@BAMTM.

The statistical values, R2 and p-values, were determined to be 0.996and 0.002, respectively, when Fe_3O_4@BAMTM was employed. The p-values were examined to determine the significance of each coefficient in demonstrating the interactions between variables (Lori et al.2015). Table 3 reveals that factors are significant for the removal efficiency of CBB in aqueous solutions when Fe_3O_4@BAMTM is utilized when the p-values are less than 0.05. Therefore, the final obtained equations in terms of the coded factors are shown in Equations. (4-5)

R1 (%) = 92.1 -13.52A – 0.94B -1.36C – 5.44AB+ 0.17AC + 0.85BC-6.09A2 – 6.43B2 -2.52C2 **(4)**

Q1 (mgdye/gNC) = 7.89 +13.52A + 0.94B +1.36C + 5.44AB - 0.17AC - 0.85BC + 6.09A2 + 6.43B2 + 2.52C2 **(5)**

Where R1 represents the percentage of CBB removal, while Q1 denotes the adsorption capacities of CBB using Fe_3O_4@BAMTM, measured in mgdye/gNC. The A, B, and C are the optimization factors, namely pH, dose (g/L), and temperature (℃), respectively (Singh et al. 2024). The experimental design matrix provides insights into the dosage, temperature and pH validities of the removal percentages and adsorption capacities.

The results demonstrated variations in performance based on the specific combination of variables, emphasizing the importance of optimizing these parameters for achieving high removal efficiency in the studied system (Abou-Melha et al. (2024). Also, the experimental design matrix provides essential information about the influences of various variables on the capturing efficiency and sorption capacity of the Fe3O4@BAMTM system. The variables considered in this study include the dosage of the material (Dose) in grams per liter (g/L), the pH, and thetemperature (Omorogie et al. 2017).

According to the obtained results, it can be observed that the removal percentages and adsorption capacities vary across different experimental conditions. For example, in rows 2 and 4, where the pH was set to 2, the removal percentages were exceptionally high, reaching 96.60% and 95.92%, respectively. These results suggest that enhancement of the removal efficiency was observed at lower pH under these specific conditions. Additionally, the dosage variations in this study significantly impact the removal percentages. For instance, the removal increases with increase the dose at pH 2 and temperature 35 ℃. Comparing rows 14 and 9, where the dose remained constant at 0.1g/L, the removal percentages differed (93.88% and 83.67%, respectively), indicating that other factors, temperature, and pH, affect the removal efficiency. The dose of 0.1 was chosen in this work due to the economic feasibility of the smallest amount of our composite (De Gisi et al. 2016). Figure (6) shows the RSM graphs of the removal percentage as a function of pH,dose, and temperature. As concluded, as discussed before, RSM was applied to optimize the three independent variables with the CCD model acquired from experimental data. To achieve removal efficiency > 90 %, the optimum predicted values of variables were pH = 2 and initial dose, g/L = 0.1 and Temperature 35℃. Implementation of the experiments under this optimal condition resulted in the very similar removal % (predicted 95.9% and experimental 96.60%), which exhibited the favorability of the CCD model for the optimization of the removal of days onto Fe_3O_4@BAMTM process (Velusamy et al. 2021).

Table 2. Experimental design for Coomassie Brilliant Blue removal using magnetic Fe_3O_4@BAMTM NCs.

No.	Coded Value			Real Value			Removal (%)	Qe (mg_{dye}/g_{NC})
	pH	Dose (g/L)	Temperature (℃)	pH	Dose (g/L)	Temperature (℃)		
1	2	0.8	50	-1	0	+1	93.88	6.12
2	2	1.5	35	-1	+1	0	96.60	3.40
3	10	1.5	35	+1	+1	0	54.42	45.58
4	2	0.8	20	-1	0	-1	95.92	4.08
5	10	0.8	50	+1	0	+1	71.43	28.57
6	6	0.8	35	0	0	0	88.44	11.56
7	6	0.8	35	0	0	0	92.52	7.48
8	6	0.1	50	0	-1	+1	78.23	21.77
9	6	0.1	20	0	-1	-1	83.67	16.33
10	6	0.8	35	0	0	0	93.20	6.80
11	6	0.8	35	0	0	0	93.20	6.80
12	6	1.5	20	0	+1	-1	86.39	13.61
13	6	1.5	50	0	+1	+1	84.35	15.65
14	2	0.1	35	-1	-1	0	93.88	6.12
15	10	0.1	35	+1	-1	0	73.47	26.53
16	10	0.8	20	+1	0	-1	72.79	27.21
17	6	0.8	35	0	0	0	93.20	6.80

Table 3. ANOVA analysis of the quadratic polynomial and cubic models for Coomassie Brilliant Blue removal efficiency and adsorption capacity using magnetic 5,5'-methylenebis (4- amino-4H-1,2,4-triazole-3-thiol) NCs.

Removal efficiency, %							Adsorption capacity, mg/g					
Source	Sum of square	df	Mean	F-value	p-value		Source	Sum of square	df	Mean	F-value	p-value	
Model	2859.75	9	317.75	5.17	0.0208	significant	Model	7234.07	9	803.79	125.01	< 0.0001	significant
A-pH	1300.77	1	1300.77	21.15	0.0025		A-pH	40.66	1	40.66	6.32	0.0401	
B-Dose	295.54	1	295.54	4.81	0.0645		B-Dose	5276.2	1	5276.2	820.61	< 0.0001	
C-Temperature	84.36	1	84.36	1.37	0.2798		C-Temperature	16	1	16	2.49	0.1587	
AB	113.1	1	113.1	1.84	0.2172		AB	9.12	1	9.12	1.42	0.2726	
AC	22.17	1	22.17	0.3606	0.5671		AC	0.3465	1	0.3465	0.0539	0.8231	
BC	1.82	1	1.82	0.0296	0.8683		BC	21.24	1	21.24	3.3	0.112	
A^2	303.74	1	303.74	4.94	0.0616		A^2	2.33	1	2.33	0.362	0.5664	
B^2	606.18	1	606.18	9.86	0.0164		B^2	1851.76	1	1851.76	288.01	< 0.0001	
C^2	46.45	1	46.45	0.7554	0.4136		C^2	20.76	1	20.76	3.23	0.1154	
Residual	430.44	7	61.49				Residual	45.01	7	6.43			
Lack of Fit	402.09	3	134.03	18.91	0.008	significant	Lack of Fit	44.56	3	14.85	134.14	0.0002	significant
Pure Error	28.35	4	7.09				Pure Error	0.443	4	0.1107			
Cor Total	3290.19	16					Cor Total	7279.08	16				

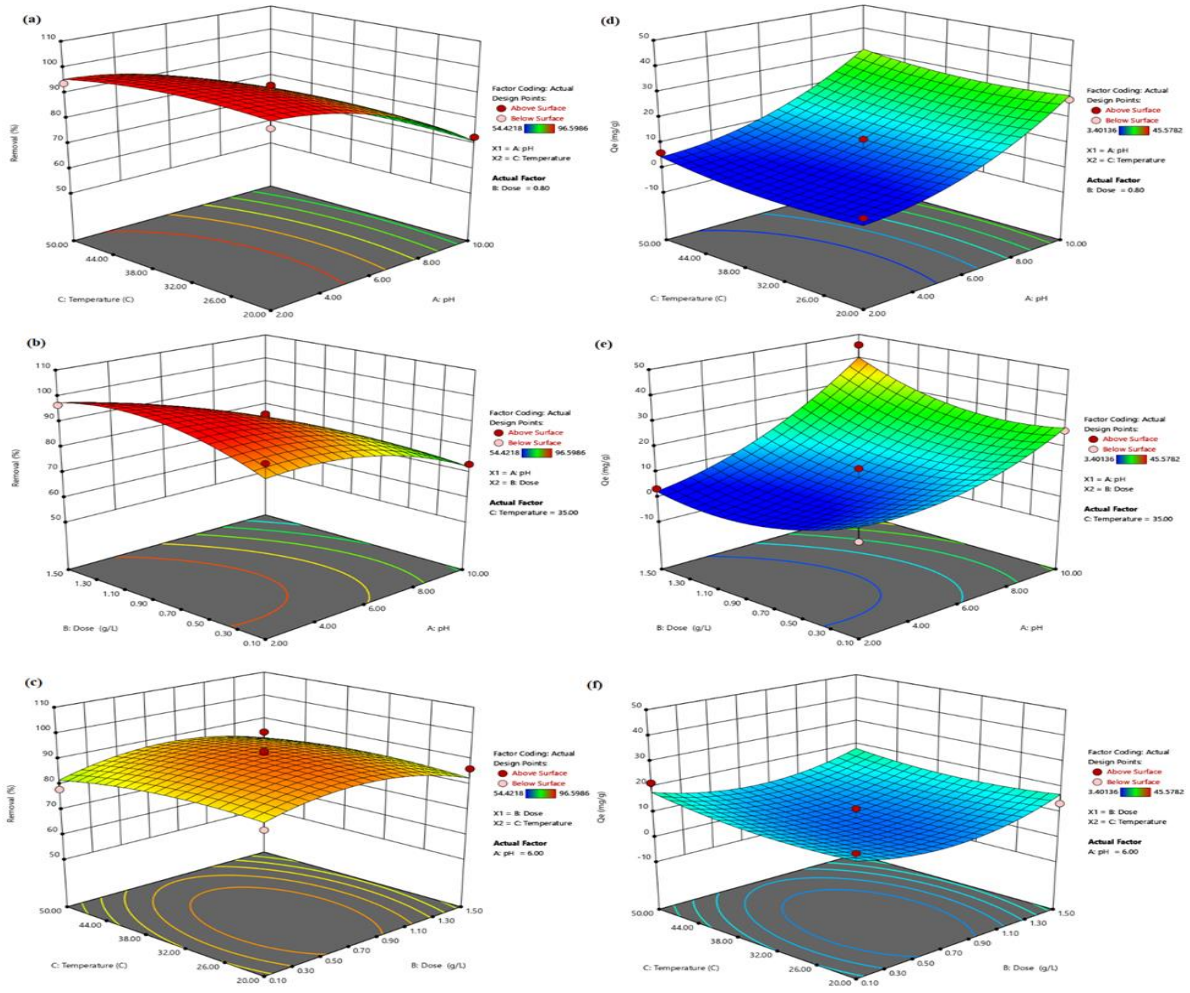

Figure 9. RSM 3D plots for the Coomassie Brilliant Blue removal using magnetic Fe_3O_4@BAMTM.

Conclusions

In this study, we successfully created a new nanocomposite Fe_3O_4@BAMTM, which proved to be highly effective in removing coomassie brilliant blue r-250 (CBB) dye from wastewater. The nanocomposite also exhibited the capability to eliminate iron (III) and NO_3^- ions. To enhance the removal of CBB dye from water using the newly synthesized nanocomposite, we employed adsorption processes and RSM (response surface methodology) with BBD (Box-Behnken design) optimization techniques.

References

Abou-Melha, Khlood (2024) Effective elimination of Coomassie Brilliant Blue dye from aqueous solutions using Cerium Metal-Organic Frameworks: Synthesis, characterization, and optimization of adsorption process utilizing Box-Behnken design. Journal of Water Process Engineering.

Ajala EO, Aliyu MO, Ajala MA (2019) Adsorption of lead and chromium ions from electroplating wastewater using plantain stalk modified by amorphous alumina developed from waste cans. Sci Rep 14, 6055 (2024).

Ciğeroğlu Z, El Messaoudi N, Şenol Z, Başkan G, Georgin, J, Gubernat, S (2024) Clay-based nanomaterials and their adsorptive removal efficiency for dyes and antibiotics: A review. Materials Today Sustainability. 26, 100735.

Dad KF. Zhao R. Hassan K. Javed H, Nawaz MU, Saleem T, Nawaz (2022) Pesticides uses, impacts on environment and their possible remediation strategies. A review. Pakistan Journal of Agricultural Research, 35(2): 274-284.

De Gisi, Lofrano, Grassi, Notarnicola, (2016) Characteristics and adsorption capacities of low-cost sorbents for wastewater treatment: A review. Sustainable Materials and Technologies.

Foo KY, Hameed B (2010) An overview of dye removal via activated carbon adsorption process. Desalination and Water Treatment - DESALIN WATER TREAT. 19. 255-274.

Gulyás N, Al-Tayawi A, Horváth Z, László, Z, Kertész Sz, Hodúr C (2023) Methods for experimental design, central composite design and the Box-Behnken design, to optimise operational parameters: A review. Acta Alimentaria. 52..

Hou X, Jones B (2006) Inductively Coupled Plasma/Optical Emission Spectrometry. https://doi.org/ 10.1002/9780470027318.a5110.

Khuri A, Mukhopadhyay S (2010) Response Surface Methodology. Wiley Interdisciplinary Reviews: Computational Statistics. 2. 128 - 149. 10.1002/wics.73.

Kılıç Z (2020) The importance of water and conscious use of water. International Journal of Hydrology, 4(5), 239–241.

Kerru N, Gummidi L, Suresh M, Sreekantha B, Jonnalagadda S B A (2020) Review on Recent Advances in Nitrogen-Containing Molecules and Their Biological Applications, Molecules

Liu F, Wu J, Chen K, Xue D (2010) Morphology Study by Using Scanning Electron Microscopy. Microscopy: Science, Technology, Applications and Education Microscopy: Science, Technology, Applications and EducationA. Méndez-Vilas and J. Díaz (Eds).

Lori N, Eydokia P, Vassilis Z, Christos N Papandreou (2015) Magnetic Nanoparticles in Medical Diagnostic Applications: Synthesis, characterization and proteins conjugation, - Current Nanoscience 12(999):1-1;

Mahmoud SA, Ghani D, Idris WA (2011) Cationic and Anionic Dye Adsorption by Agricultural Solid Wastes: A Comprehensive Review. Desalination. 280. 1-13. https://doi.org/10.1016/j.desal.2011.07.019.

Mahmood I, Imadi S, Shazadi K., Gul, A., Hakeem, KR. (2015). Effects of Pesticides on Environment,

Mustafa M. Abdulrasool, Alaa H. Jawad, JKS (2012) Synthesis, Characterization and Evaluation of Biological Activity of New Heterocyclic Compounds Containing 1, 2, 4- Triazoleand 1,3,4-Thiadiazole Rings. International Journal of Applied Science and Technology, 2(10), 157.

Mohamed FM, El-Aassar MR, Ibrahim OM, Elsayed A, Alrakshy MF, Abdel Rafea M, Omran KA. (2024) Effective Removal of Carcinogenic Azo Dye from Water Using Zea mays-Derived Mesoporous Activated Carbon. ACS Omega. 2024 Mar 4;9(11):13086-13099.

Njum A (2017) Adsorption Technology for Removal of Toxic Pollutants. In: Rene, E., Sahinkaya, E., Lewis, A, Lens, P. (eds) Sustainable Heavy Metal Remediation. Environmental Chemistry for a Sustainable World. Springer, Cham.

Omorogie M, Naidoo E, Ofomaja A (2017) Response surface methodology, central composite design, process methodology and characterization of pyrolyzed KOH pretreated environmental biomass: mathematical modelling and optimization approach. Modeling Earth Systems and Environment.

Ostertagova E (2012) Modelling Using Polynomial Regression. Procedia Engineering. 48. 500–506. https://doi.org/10.1016/j.proeng.2012.09.545.

Programme United Nations Environment. (2016) A Snapshot of the World's Water Quality: Towards a global assessment. United Nations Environment Programme, Nairobi, Kenya. 162pp. A Snapshot of the World's Water Quality (p. 162).

Rahman Md H, Prakash B (2021) An Overview of Non-biodegradable Bio plastics. Journal of Cleaner Production. 294. 126218. 10.1016/j.jclepro.2021.126218.

Shayo GM, Elimbinzi E, Shao GN (2023) Severity of waterborne diseases in developing countries and the effectiveness of ceramic filters for improving water quality. Bull Natl Res Cent 47, 113 .

Sawyer S (2009) Analysis of Variance: The Fundamental Concepts. Journal of Manual & Manipulative Therapy. 17. 27E-38E.https://doi.org/ 10.1179/jmt.2009.

Sevim F, Demir F, LAÇİN Ö, ERKILIÇ Ö (2024) Investigation of Adsorption Capacity, Kinetics and Thermodynamics in The Removal of Textile Dye in Wastewater. https://doi.org/10.21203/rs.3.rs-4261649/v1.

Singh J, Bhattu M, Verma M (2024) Rice Straw Derived Mesoporous Biochar for the Removal of Coomassie Brilliant Blue Dye. Topics in Catalysis. 1-10., https://doi.org/ 10.1007/s11244-024-01961-5.

Shayo GM., Elimbinzi E, Shao GN, Fabian C (2023) Severity of waterborne diseases in developing countries and the effectiveness of ceramic filters for improving water quality. Bulletin of the National Research Centre,47(1).

Velusamy S, Roy A, Sundaram S, Mallick, T (2021) A Review on Heavy Metal Ions and Containing Dyes Removal Through Graphene Oxide-Based Adsorption Strategies for Textile Wastewater Treatment. Chemical record (New York, N.Y.). 21.

Yuan N, Cai H, Liu T, Huang Q, Zhang X (2019) Adsorptive removal of methylene blue from aqueous solution using coal fly ash-derived mesoporous silica material. Adsorption Science and Technology. 37. 333-348.

Zhang F, Yin X, Lan J, Zhang, W (2016) Application of Ba3 (PO4)2/Fe_3O_4 as a novel magnetic adsorbent to remove methyl blue from aqueous solution. Journal of Materials Science. 51AboMarkeb A, Moral-Vico J, Antoni S, Xavier F(2023) Optimization of lead (II) removal from water and wastewater using a novel magnetic nanocomposite of amino propyl triethoxysilane coated with carboxymethyl cellulose cross-linked with chitosan nanoparticles, Arabian Journal of Chemistry16 (8), 105022;